Supplementary Information (SI) for Materials Chemistry Frontiers.
This journal is © the Partner Organisations 2026

Supplementary Information

Organic–Inorganic Heterojunction Photoanode for Photoelectrochemical Conversion of Glycerol to Dihydroxyacetone

Chen Gong,[a] Zeju Li,[a] Jian Dai,[a] Hongxia Ning,[a] Peili Zhang,[a] Ming Cheng,[b] Shudong Zhang,[b] Fusheng Li[a, b]*

[a] State Key Laboratory of Fine Chemicals, Frontier Science Center for Smart Materials, School of Chemical Engineering, Dalian University of Technology, 116024 Dalian, China.
[b] SINOPEC (Dalian) Research Institute of Petroleum and Petrochemicals Co., Ltd. 116045 Dalian, Liaoning, China. E-mail: lifusheng.fshy@sinopec.com

Supplementary Figures

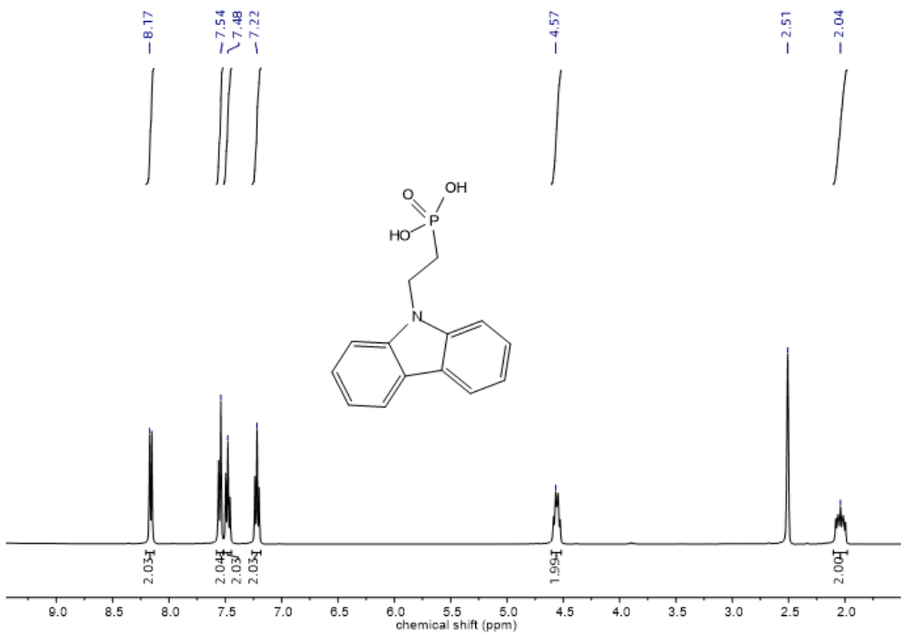

Figure S1. ^{1}H NMR spectrum of 2PACz.

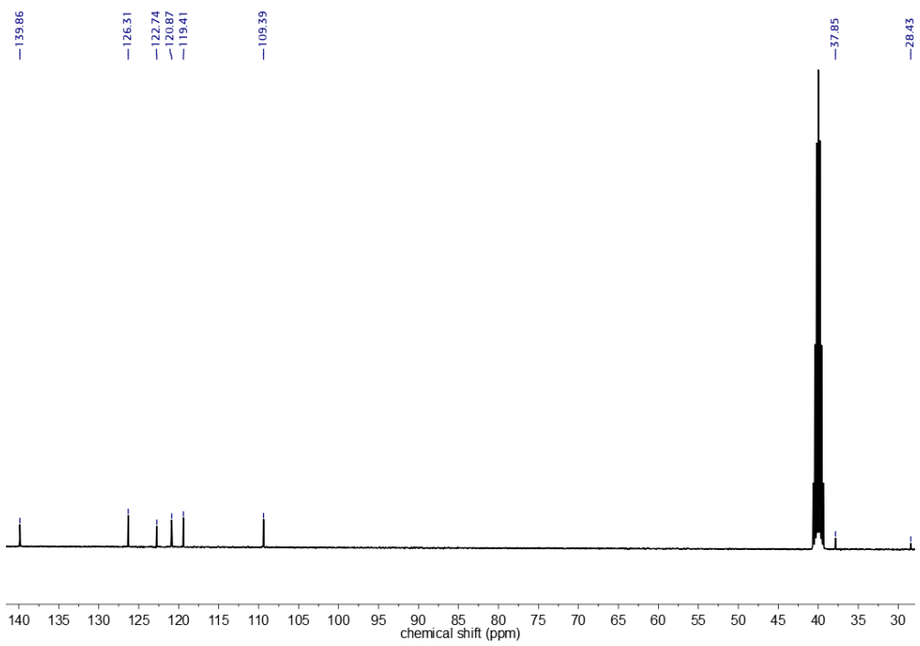

Figure S2. ^{13}C NMR spectrum of 2PACz.

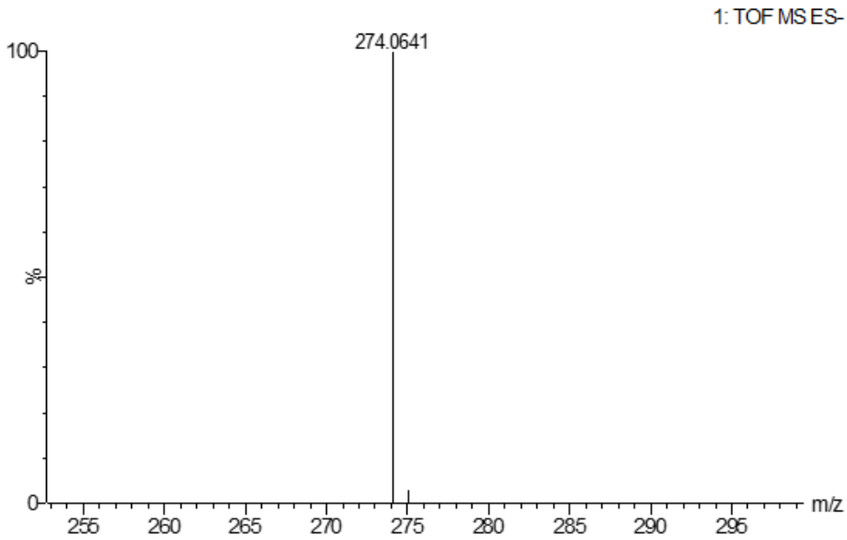

Figure S3. Electrospray mass spectrum of 2PACz.

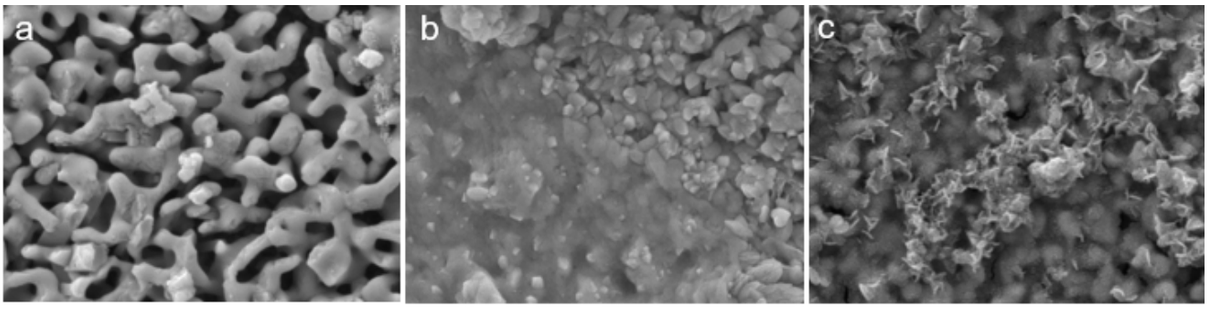

Figure S4. Digital photographs and scanning electron microscope (SEM) images of (a) BVO, (b) 2PACz/BVO, and (c) FeOOH/2PACz/BVO.

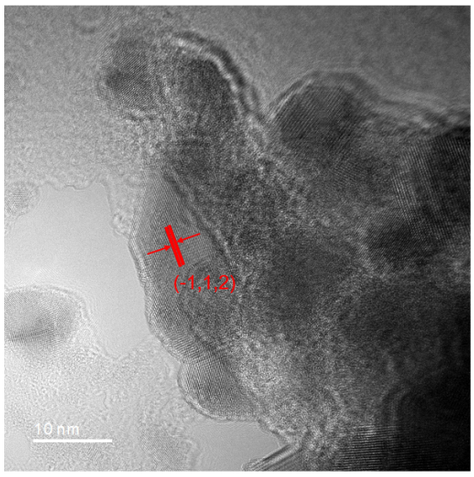

Figure S5. High-resolution TEM images of BVO.

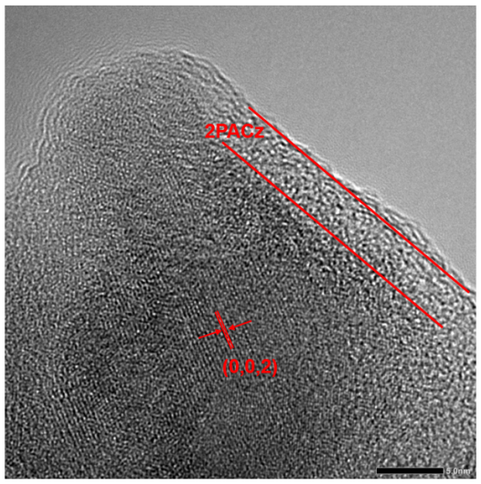

Figure S6. High-resolution TEM images of 2PACz/BVO.

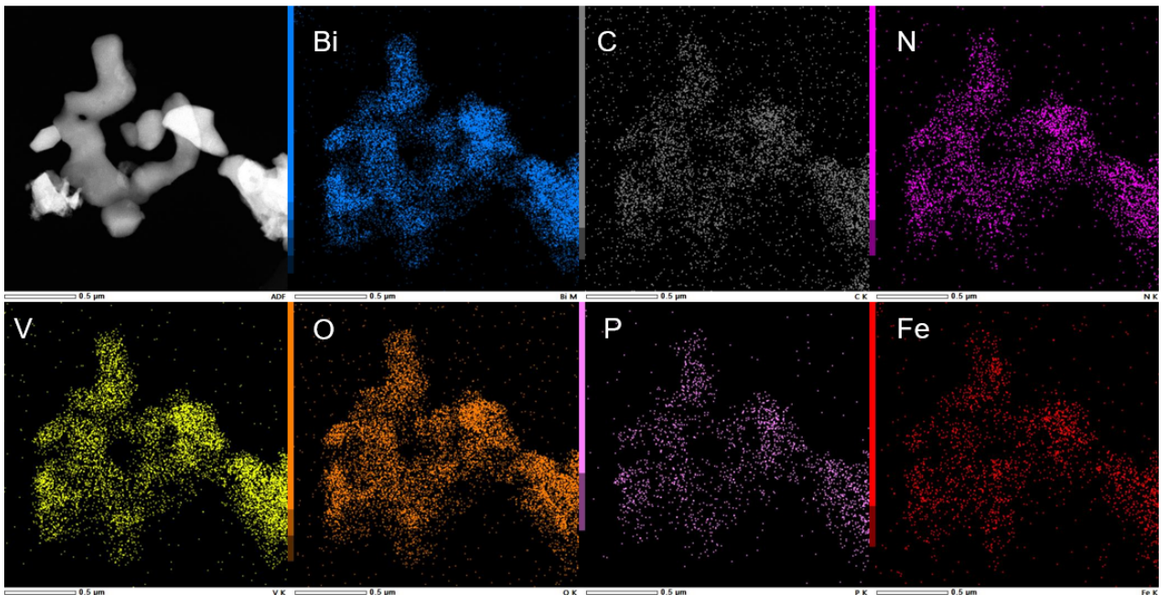

Figure S7. HAADF-STEM and the corresponding EDS elemental mappings for FeOOH/2PACz/BVO.

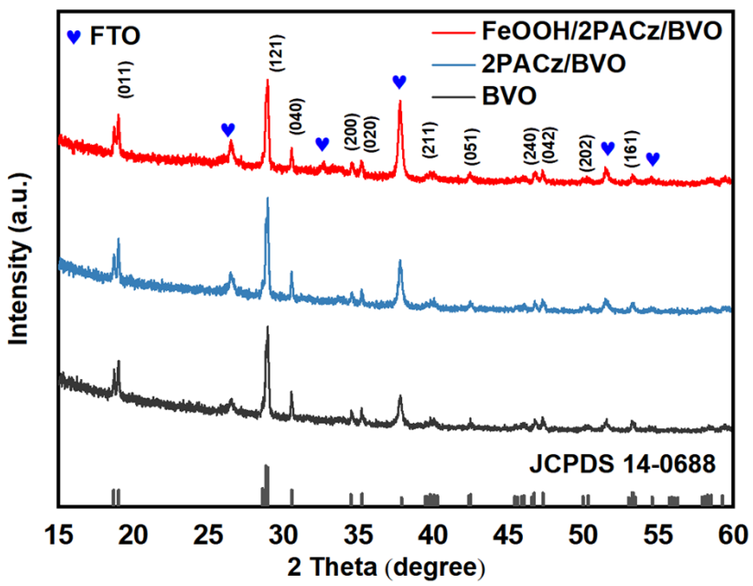

Figure S8. XRD pattern of BVO, 2PACz/BVO, and FeOOH/2PACz/BVO.

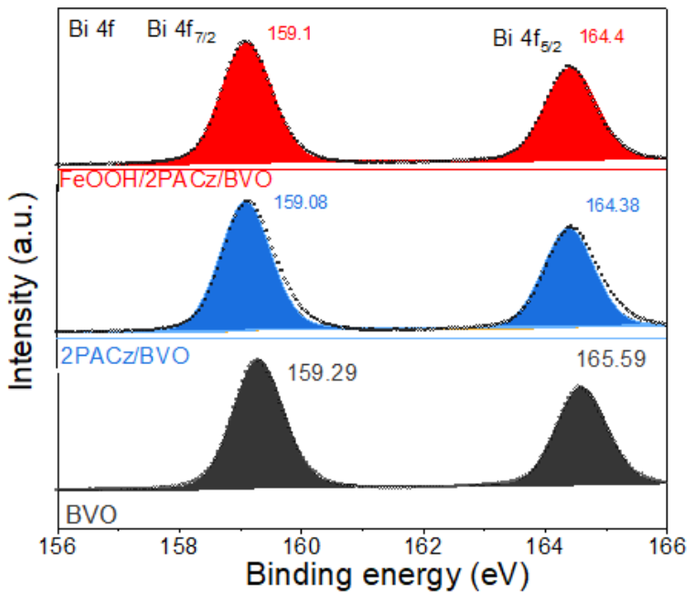

Figure S9. XPS of the Bi 4f for BVO, 2PACz/BVO, and FeOOH/2PACz/BVO.

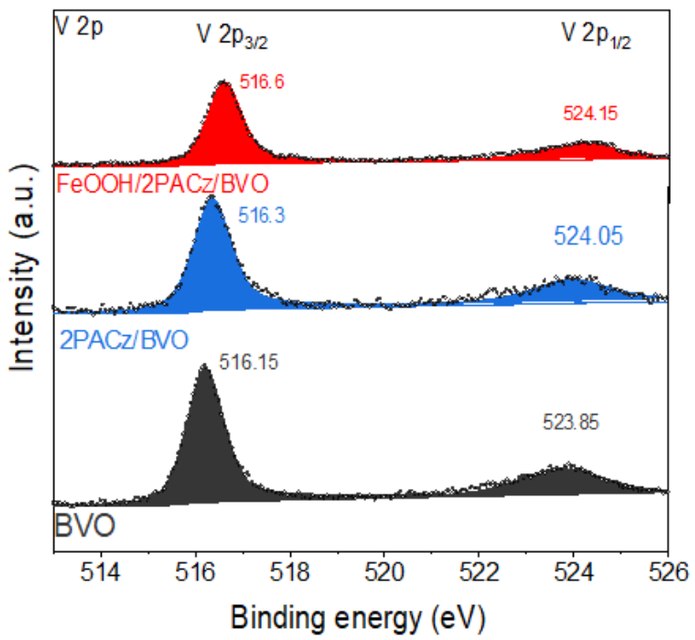

Figure S10. XPS of the V 2p for BVO, 2PACz/BVO, and FeOOH/2PACz/BVO.

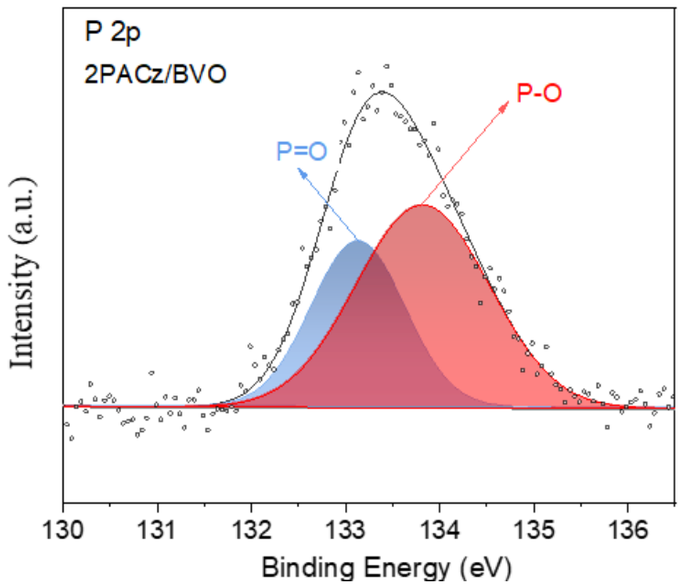

Figure S11. XPS of the P 2p for 2PACz/BVO.

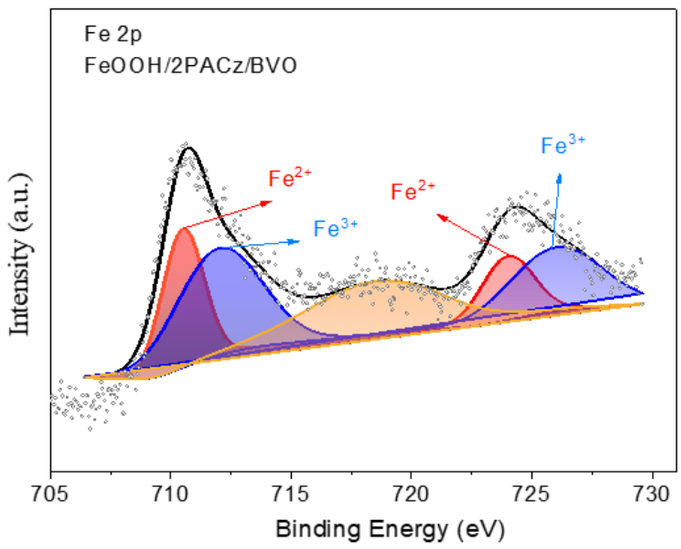

Figure S12. XPS of the Fe 2p for FeOOH/2PACz/BVO.

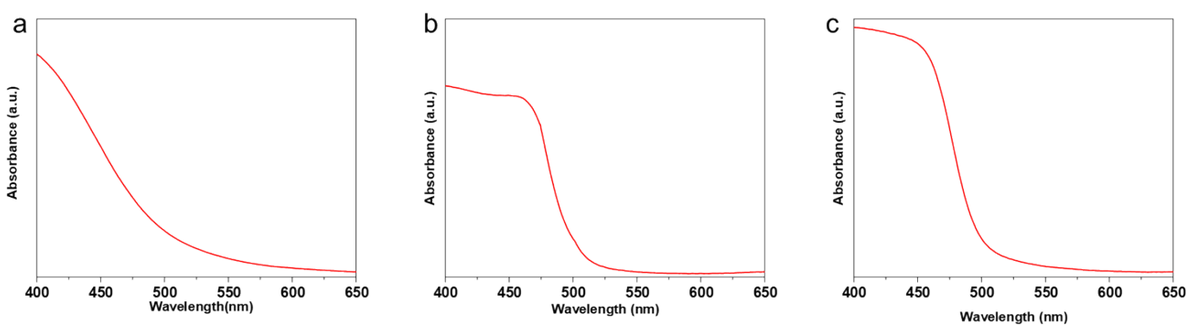

Figure S13. UV-vis of (a) 2PACz/FTO, (b) BVO/FTO, (c)2PACz/BVO/FTO.

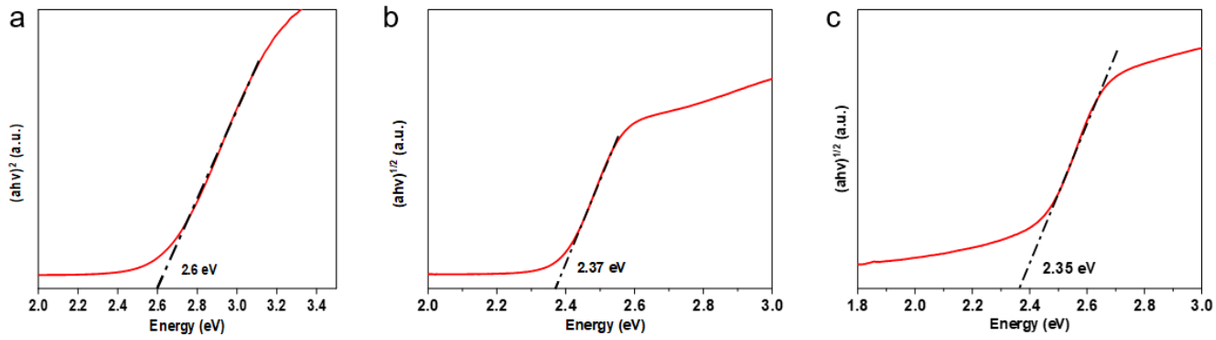

Figure S14. Tauc curves of (a) 2PACz/FTO, (b) BVO/FTO, (c)2PACz/BVO/FTO.

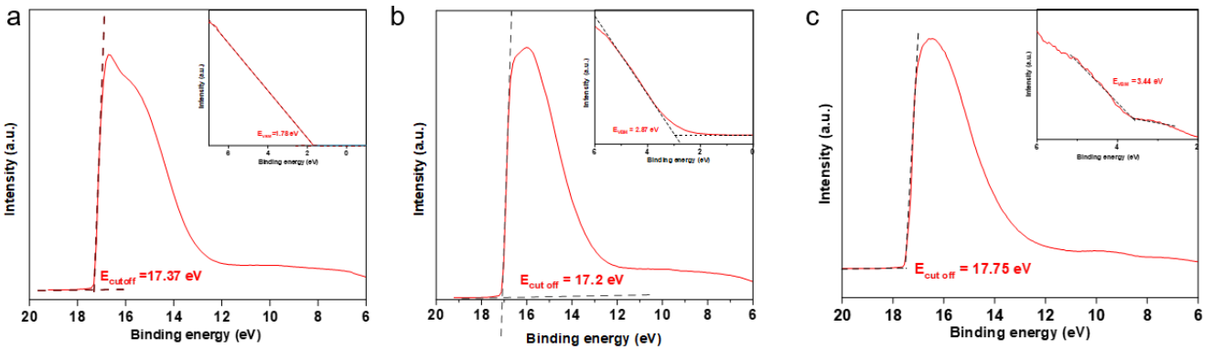

Figure S15. UPS spectrum of (a) 2PACz/FTO, (b)BVO/FTO, (c)2PACz/BVO/FTO.

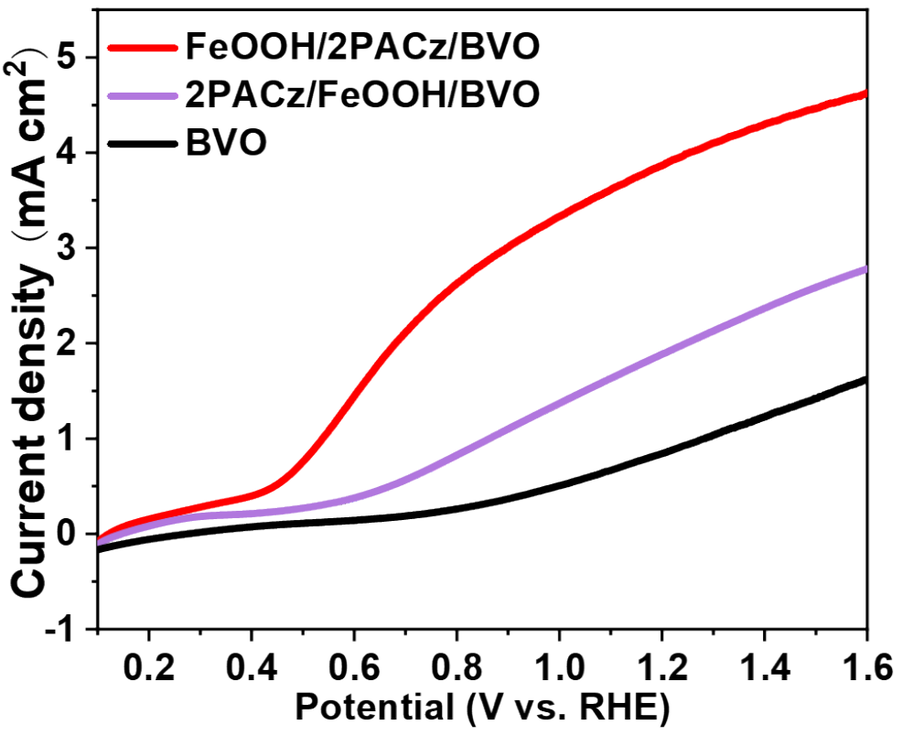

Figure S16. Linear sweep voltammetry (LSV) curves of BVO, FeOOH/2PACz/BVO, and 2PACz/FeOOH/BVO photoanodes measured in 0.2 M Na_2SO_4 with 0.5 M glycerol.

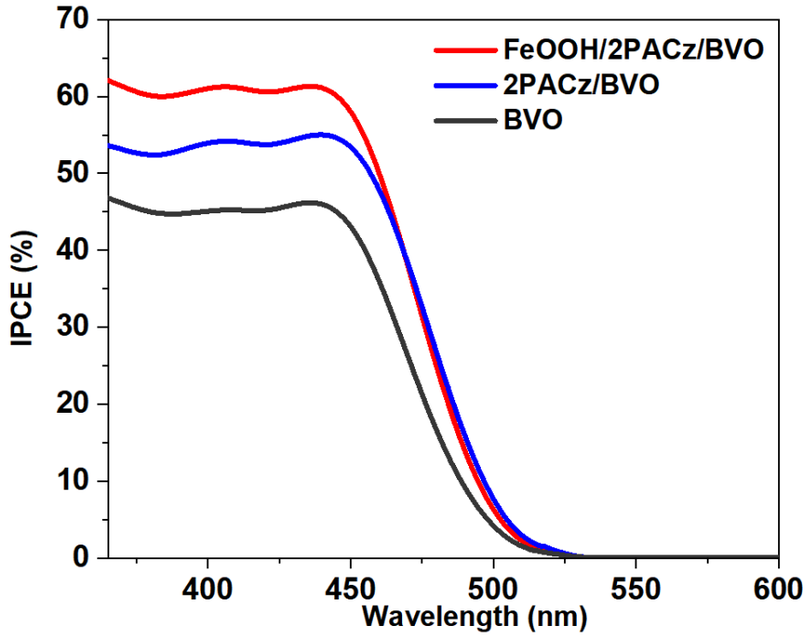

Figure S17. IPCE spectra of BVO, 2PACz/BVO, and FeOOH/2PACz/BVO at 1.2 V *vs*. RHE in 0.2 M Na_2SO_4 electrolyte with 0.5 M GLY.

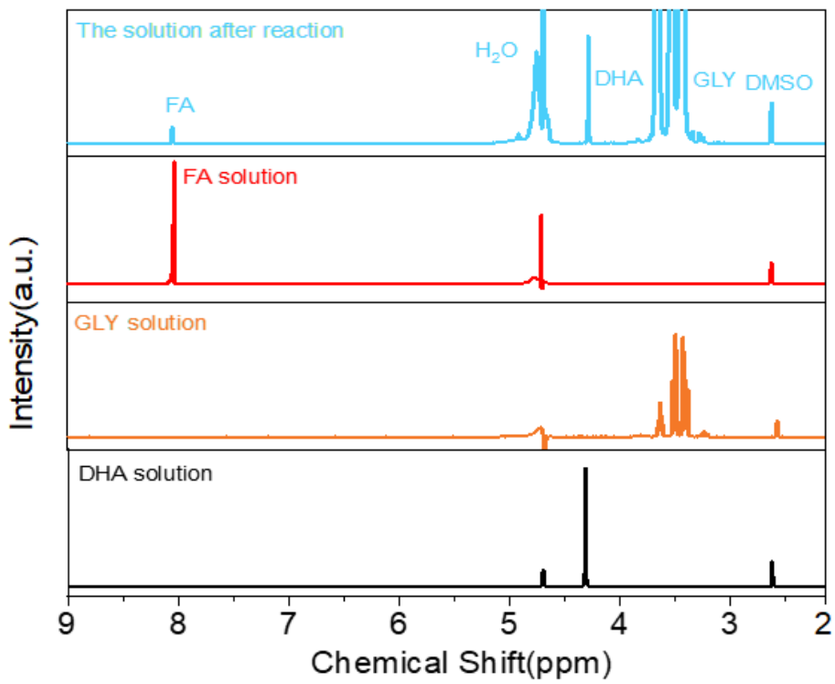

Figure S18. Typical ^{1}H NMR spectra of the FeOOH/2PACz/BVO electrolyte after 3 hours of reaction under light at 1.2 V *vs*. RHE, with DMSO as an internal standard, and typical ^{1}H NMR spectra of FA, DHA, and GLY.

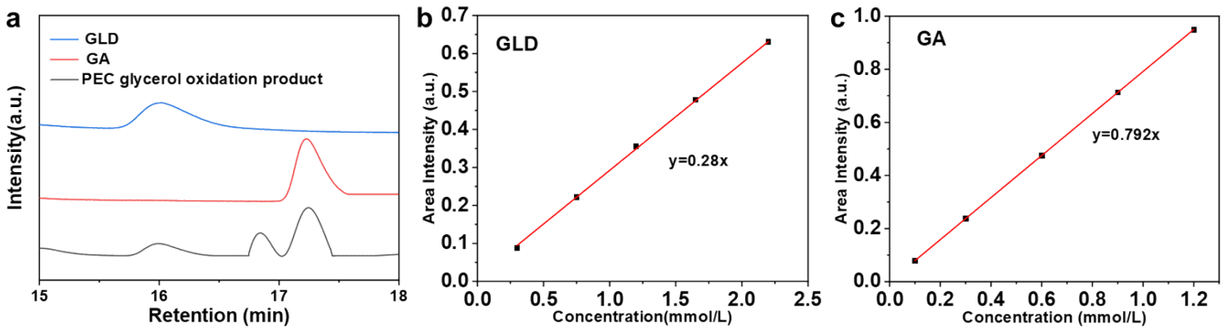

Figure S19.(a) Liquid chromatography analysis of glyceraldehyde (GLD) and glycolic acid (GA), (b) Standard curve of GLD, (c) Standard curve of GA

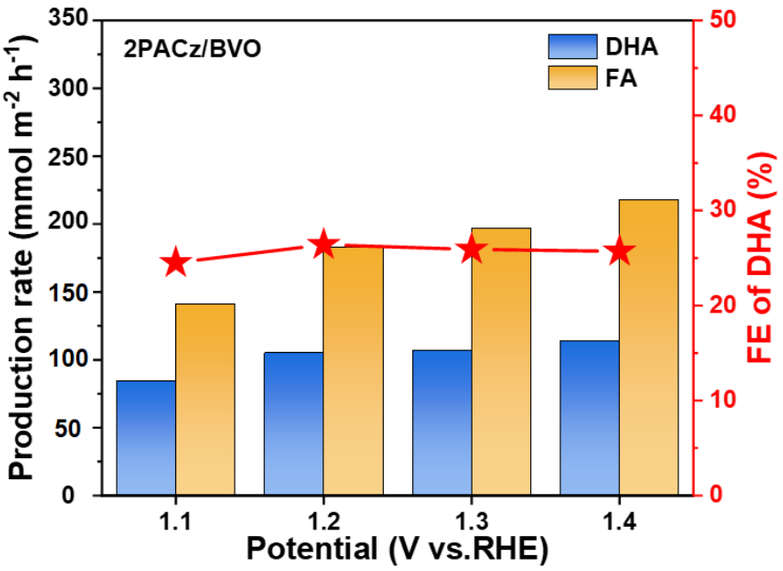

Figure S20. Production formation rates and total FEs of 2PACz/BVO at different potentials in 0.2 M Na_2SO_4 electrolyte with 0.5 M GLY.

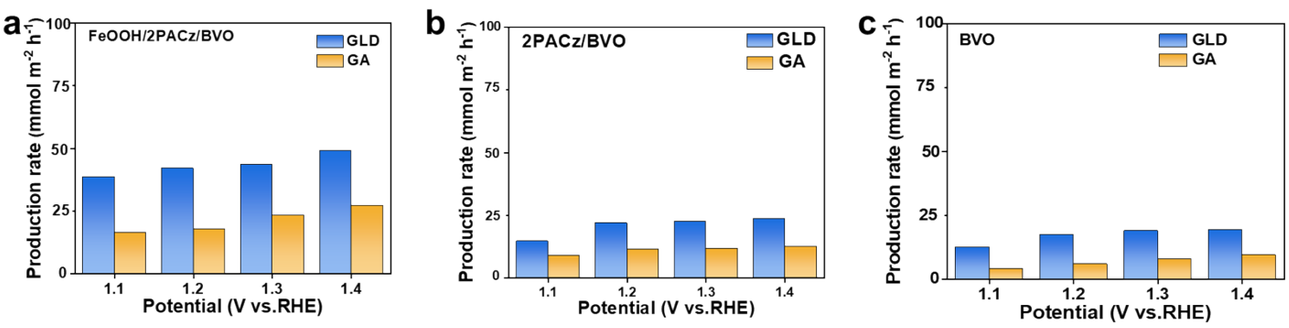

Figure S21.The yields of GLD and GA on (a) FeOOH/2PACz/BVO, (b) 2PACz/BVO, and (c) BVO photoanodes

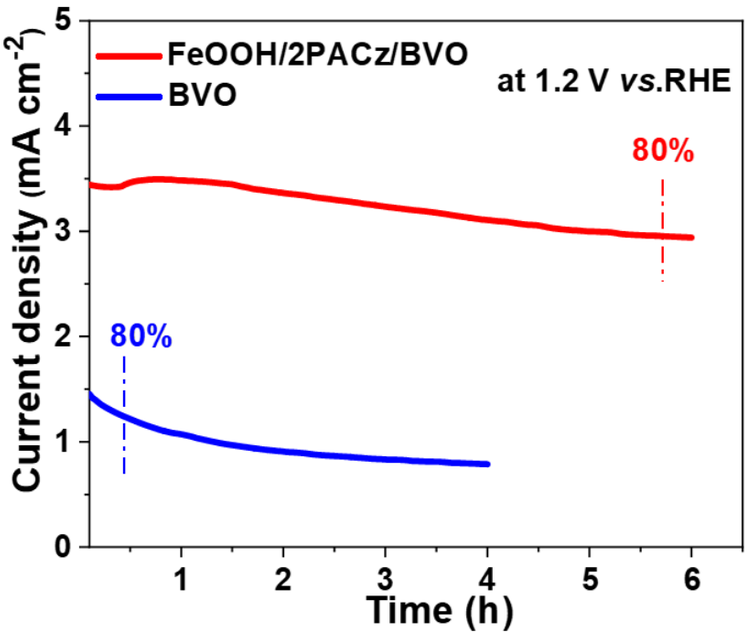

Figure S22. Photocurrent density-time curves of BVO, FeOOH/2PACz/BVO at 1.2 V *vs*. RHE in 0.2 M Na_2SO_4 electrolyte with 0.5 M GLY.

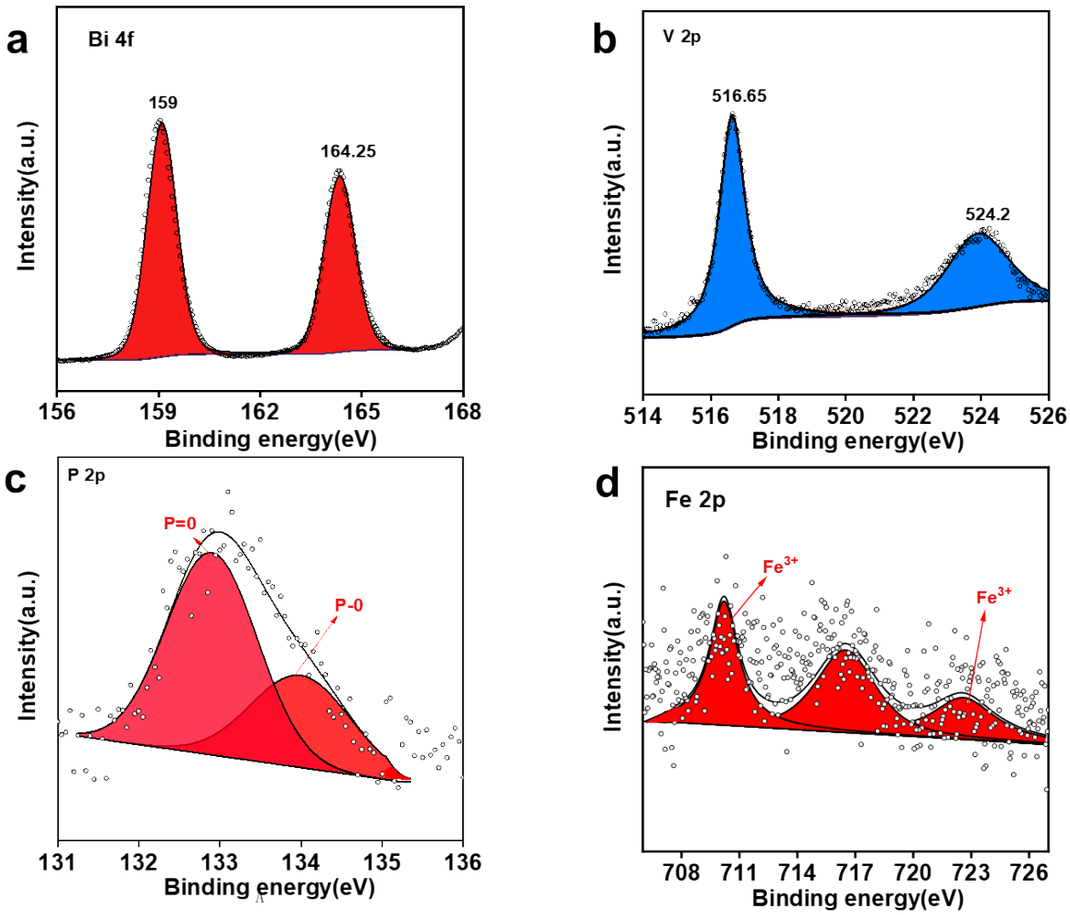

Figure S23.XPS spectra of (a) Bi 4f, (b) V 2p, (c) P 2p, and (d) Fe 2p for the post-reaction FeOOH/2PACz/BVO photoanode.

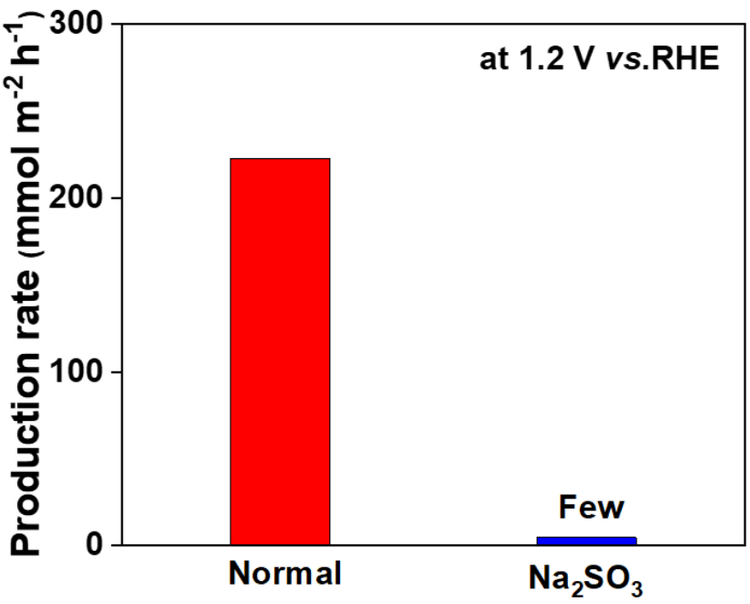

Figure S24. The production rate of DHA in the presence of various radical scavengers over the FeOOH/2PACz/BVO photoanode at 1.2 V *vs*. RHE in 0.2 M Na_2SO_4 electrolyte with 0.5 M GLY.

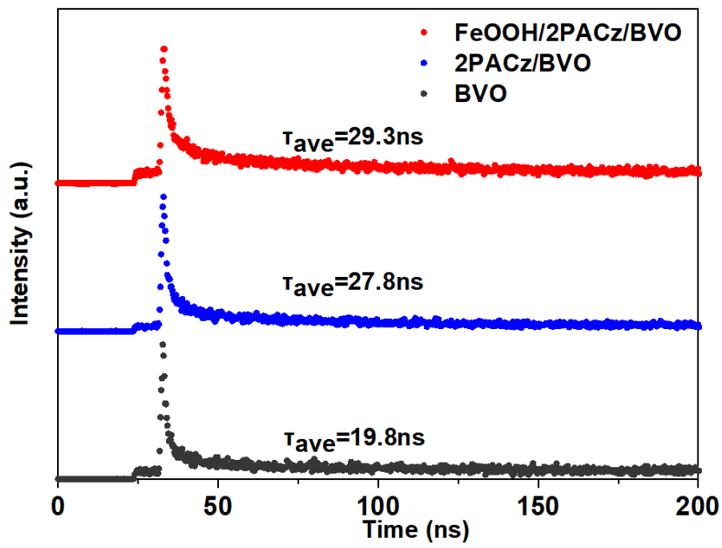

Figure S25. Time-resolved photoluminescence decay spectra of BVO, 2PACz/BVO, and FeOOH/2PACz/BVO.

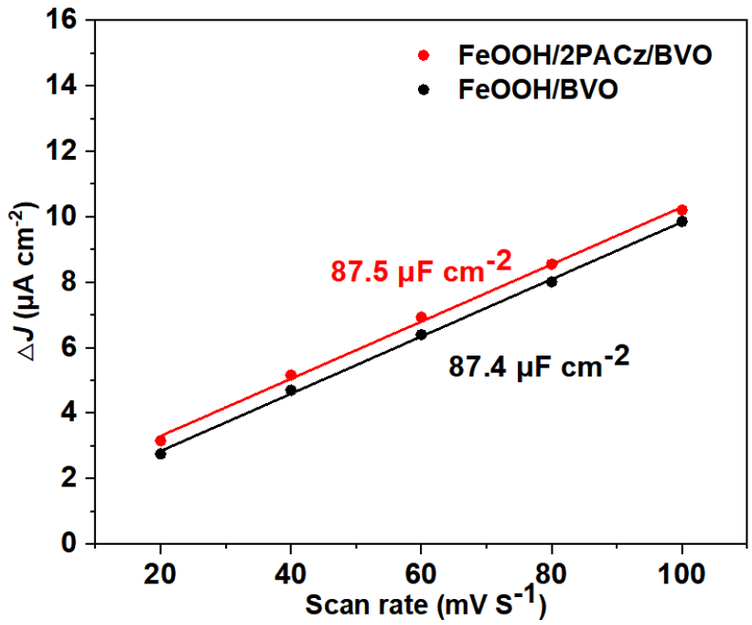

Figure S26. Fitting curve of electrochemical double-layer capacitances in 0.2 M Na_2SO_4 electrolyte with 0.5 M GLY. The scanning potential range is from −0.05 V to 0.05 V *vs*. RHE.

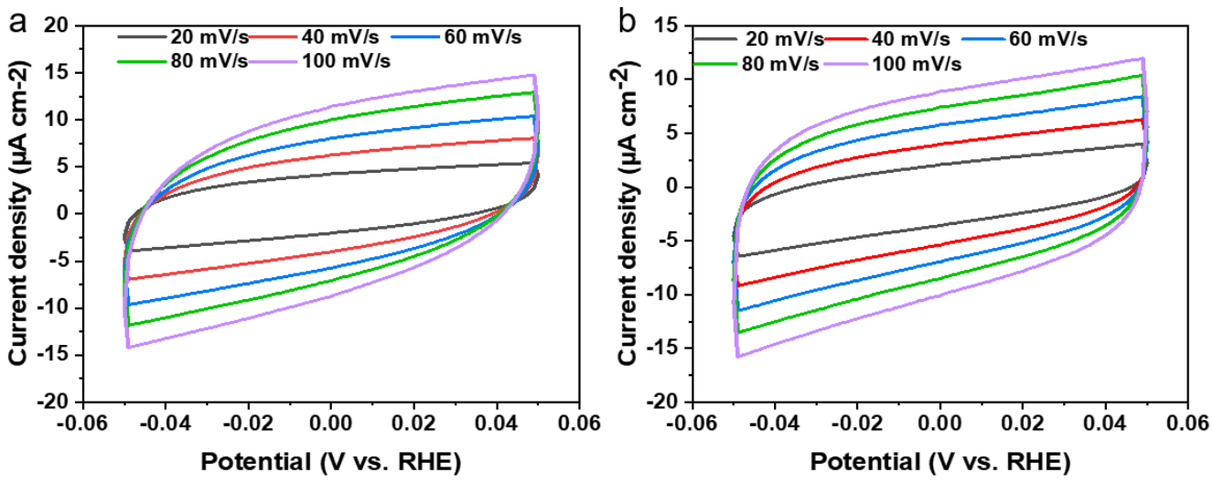

Figure S27 Cyclic voltammograms of (a) FeOOH/2PACz/BVO and (b) FeOOH/BVO photoanodes were measured at the scan rates: 20, 40, 60, 80, 100 mV s^{-1} in 0.2 M Na_2SO_4 electrolyte with 0.5 M GLY. The scanning potential range is from −0.05 V to 0.05 V *vs*. RHE.

Table S1. Total Faradaic efficiency of FeOOH/2PACz/BVO

Voltage/V	Total Faradaic efficiency/%	the total carbon balance/%
1.1	85.8	85
1.2	88.3	86
1.3	89.4	88
1.4	90.2	89

Table S2. Comparison of PEC glycerol oxidation performance on $BiVO_4$-based photoanodes

Photoanode	pH	Photocurrent density (mA cm^{-2})	DHA Faradaic efficiency (%)	Reference
FeOOH/2PACz/BVO	6.8	3.9	40.2	This work
$BiVO_4$ via N_2 treatment	2.0	4.0	35.0	[1]
Pd/BVO	7.0	2.5	N/A	[2]
BVO	7.0	2.5	20.0	[3]

Table S3. Impedance of FeOOH/2PACz/BVO and FeOOH/BVO

Photoanode	R_s/Ω	R_{bulk}/Ω	C_{bulk}/μF	R_{ct}/Ω	C_H/nF
FeOOH/2PACz/BVO	31.6	251	14.86	9.3	589.8
FeOOH/BVO	35	446	12.9	10.1	439.22

Reference:

[1] Y. Lee, Y. Jo and Y. J. Jang, *Journal of Materials Chemistry C* 2025, **13**, 1301-1309.

[2] J. Xie, B. Tam, Y. Cai, L. Li, Z. Lin, K. Lambrecht, A. A. Bakulin and A. Kafizas, *Inorganic Chemistry Frontiers* 2025, **12**, 8785-8799.

[3] D. Liu, J.-C. Liu, W. Cai, J. Ma, H. B. Yang, H. Xiao, J. Li, Y. Xiong, Y. Huang and B. Liu, *Nature Communications* 2019, **10:**1779.